

# Effect of machining parameters on surface integrity of silicon carbide ceramic using end electric discharge milling and mechanical grinding hybrid machining<sup>†</sup>

Renjie Ji, Yonghong Liu\*, Yanzhen Zhang, Baoping Cai, Xiaopeng Li and Chao Zheng

*College of Electromechanical Engineering, China University of Petroleum, Shandong, 266580, China*

(Manuscript Received April 20, 2012; Revised July 25, 2012; Accepted August 22, 2012)

## Abstract

A novel hybrid process that integrates end electric discharge (ED) milling and mechanical grinding is proposed. The process is able to effectively machine a large surface area on SiC ceramic with good surface quality and fine working environmental practice. The polarity, pulse on-time, and peak current are varied to explore their effects on the surface integrity, such as surface morphology, surface roughness, micro-cracks, and composition on the machined surface. The results show that positive tool polarity, short pulse on-time, and low peak current cause a fine surface finish. During the hybrid machining of SiC ceramic, the material is mainly removed by end ED milling at rough machining mode, whereas it is mainly removed by mechanical grinding at finish machining mode. Moreover, the material from the tool can transfer to the workpiece, and a combination reaction takes place during machining.

*Keywords:* End electric discharge milling; Machining performance; Mechanical grinding; Silicon carbide ceramic; Surface integrity

## 1. Introduction

Silicon carbide (SiC) ceramic has been widely used in modern industry. With the exceptional hardness, wear resistance and high mechanical strength, it is becoming very desirable for a number of applications such as heat exchangers, gas turbines, high temperature bearings, seals and furnaces [1-4]. However, the machining of SiC ceramic is difficult and expensive due to its brittleness and high hardness. Grinding of SiC ceramic is the primary traditional machining method used in achieving the desired tolerances and surface integrity, but the process shows low machining efficiency [5, 6].

To overcome technical difficulties in machining this material, nontraditional machining methods, such as water jet machining, laser beam machining and ultrasonic machining, are employed [7-9]. They can achieve a fairly high material removal rate, but are often accompanied by some surface defects, which in many cases are unacceptable to a final finished product, and could undermine the fatigue strength of the final product. Electrical discharge machining (EDM) is an electrical spark erosion process which removes the material by means of a series of recurring electrical sparks between an electrode and a workpiece flushed with or submerged in a dielectric fluid. Since there is no direct physical contact between the tool electrode and the workpiece, the process is able to machine any

conductive component into accurate and complex shapes regardless of its hardness [10-12].

Notwithstanding the advantages of using EDM in machining SiC ceramic, it is obvious that the problem of low efficiency has to be overcome. Reducing machining time and maintaining reasonable accuracy has always been of research interest. Recently, some researches have been made to improve the machining efficiency using EDM milling. The results show that the material removal rate can be improved proportionally, but it still can't meet the demand of modern industrial applications, and the machined surface is poor [13-15]. Ji et al. [16, 17] developed the electric discharge milling and mechanical grinding compound process, which uses a steel wheel with uniformly distributed abrasive inserts in the circumference as the tool. During this process, electric discharge milling and mechanical grinding occur alternately, and SiC ceramic can be easily machined. However, the width of the steel wheel tool is small, and the material removal rate is still low when machining a large surface area on SiC ceramic.

A novel high speed hybrid machining process that integrates end electric discharge (ED) milling and mechanical grinding to machine SiC ceramic is proposed in this paper. The process employs a turntable with several uniformly distributed small cylindrical copper electrodes and abrasive sticks as the tool. The diameter of the tool turntable is larger than the width of the steel wheel used in references [16, 17], so a large surface area on SiC ceramic can be machined at one path. The hybrid machining process shows high machining efficiency, and the material re-

\*Corresponding author. Tel.: +86 532 86983303, Fax.: +86 532 86983300

E-mail address: liuyh@upc.edu.cn; liuyhupe@126.com

<sup>†</sup>Recommended by Associate Editor Haedo Jeong

© KSME & Springer 2013

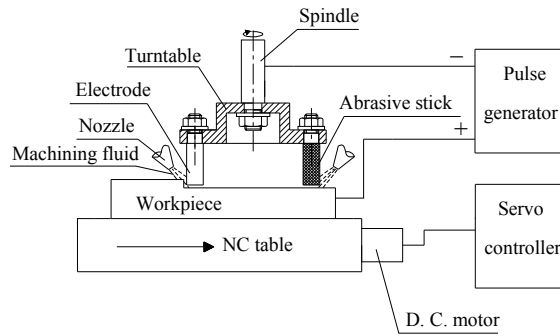


Fig. 1. Schematic illustration of end ED milling and mechanical grinding of SiC.

moval rate can reach  $130.72 \text{ mm}^3/\text{min}$ . In the present study, the SiC ceramic is machined by the new process to investigate the surface integrity, including the surface morphology, surface roughness, micro-cracks, and composition on the machined surface, under a wide range of machining conditions.

## 2. Principle of end ED milling and mechanical grinding of SiC

The principle of end ED milling and mechanical grinding of SiC ceramic is illustrated in Fig. 1. The tool and the workpiece are connected to the negative and positive poles of the pulse generator, respectively. The tool is a turntable with several uniformly distributed small cylindrical electrodes and abrasive sticks rotating rapidly around its axis. The tool is mounted onto a rotary spindle, driven by an A.C. motor. The workpiece is SiC ceramic blank and is mounted onto a numerically controlled (NC) table. The machining fluid is a water-based emulsion.

During machining, the tool rotates at a high speed, the machining fluid is flushed into the gap between the tool and the workpiece with several nozzles, and the SiC ceramic workpiece is fed towards the tool with the NC table. As the workpiece approaches the tool and the distance between the workpiece and the electrode reaches the discharge gap, electrical discharges are produced. A vapor bubble forms around this channel. The surrounding water-based emulsion restricts plasma growth and makes the plasma energy densities rise to very high levels. Petrofes and Gadalla [18] showed that the plasma temperature could reach nearly 40000K and the plasma pressure could rise to 300 MPa in EDM of conducting advanced ceramics. The instantaneous high temperature and pressure plasma cause SiC ceramic to be removed by electric discharge milling, and a modified surface layer is formed on the workpiece surface. The following abrasive stick grinds the modified surface layer. The modified surface layer can be removed easily by the abrasive stick. A large diameter turntable with several cylindrical copper electrodes and abrasive sticks is used as the tool; the tool stick is manufactured easily and shows low cost, and a large surface area can be easily machined by the hybrid process. The cylindrical electrodes and abrasive sticks are fixed on the turntable alternately, the

Table 1. Comparison of experimental results for machining of SiC ceramic with different processes.

	MRR ( $\text{mm}^3/\text{min}$ )	SR Ra ( $\mu\text{m}$ )	TWR (%)
ED milling	26.51	2.33	106.51
Hybrid machining	38.14	1.07	65.62
Mechanical grinding	4.13	0.43	470.83

machining fluid is flushed into the gap, and the chips are flushed away easily, which makes the processing stable. In addition, a water-based emulsion is used as the machining fluid, so harmful gas is not generated during machining, and the equipment is not corroded.

Compared with electric discharge (ED) milling and conventional mechanical grinding, the advantage of the hybrid machining process can be explained as follows. During ED milling of SiC ceramic, the modified surface layer will form on the workpiece surface, which makes the subsequent discharge difficult and degrades the workpiece surface quality. During conventional mechanical grinding of SiC ceramic, the grinding force is high due to the high hardness of the workpiece, so the material removal rate is low. During this hybrid machining process, mechanical grinding removes the softened material created by end electric discharge milling. Electric discharges are produced easily on the workpiece surface without modified surface layer, so end ED milling and mechanical grinding are mutually beneficial, and the higher overall machining performance can be achieved. The comparison experiments have been done, and the experimental results are shown in Table 1. From these results it is obvious that the higher material removal rate (MRR), the lower surface roughness (SR Ra) and the lower tool wear ratio (TWR) can be obtained with the hybrid machining process in comparison with ED milling alone. Furthermore, although the SR with the hybrid machining process is a little higher than that with mechanical grinding, the MRR is far higher and the TWR is far lower with the hybrid machining process in comparison with mechanical grinding.

## 3. Experimental procedures

In the following experiments, the workpiece material was SiC ceramic, the SiC sample size used for experiments was  $130 \text{ mm} \times 60 \text{ mm} \times 20 \text{ mm}$ ; its physical and mechanical properties are presented in Table 2. The tool was a turntable with eight uniformly distributed cylindrical copper electrodes and cast iron bonded diamond abrasive sticks in the circumference, as shown in Fig. 2. The copper electrodes and abrasive sticks are fixed on the turntable alternately and separately. The grit size of diamond in the abrasive sticks was #120 (grain size =  $124 \mu\text{m}$ ); the concentration of diamond in the abrasive sticks was 100%. The diameter of the cylindrical copper electrode was 10 mm, the diameter of the abrasive stick was 10 mm, the diameter of the turntable was 90 mm, and the rotational speed of the spindle was 3000 rpm. The machining fluid was a wa-

Table 2. Physical and mechanical properties of silicon carbide ceramic (Manufacturer's data).

Item	Unit	Data
Maximum service temperature	°C	1380
Density	g/cm <sup>3</sup>	3.02
Open porosity	%	< 0.1
Bending strength	Mpa	250 (20°C)
	Mpa	280 (1200°C)
Elastic modulus	Gpa	330 (20°C)
	Gpa	300 (1200°C)
Thermal conductivity	W/m-k	45 (1200°C)
Thermal expansion coefficient	K <sup>-1</sup> × 10 <sup>-6</sup>	4.5
Mohs hardness		13
Acid and alkali resistance		Excellent

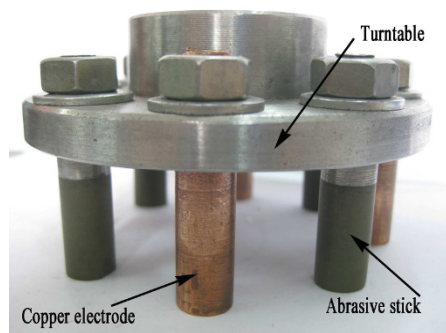


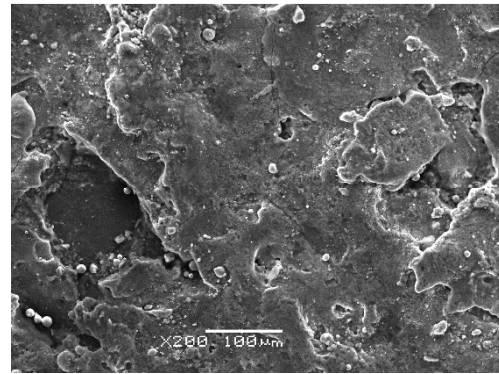
Fig. 2. Photograph of the tool used in the hybrid process.

ter-based emulsion composed of 8 mass% emulsified oil and 92 mass% distilled water, which were mixed with a constant speed power-driver mixer (JJ-2, Jintan Medical Instrument Factory, China). The flux of the machining fluid was 200 mL/s. The material removal rate (MRR) and tool wear ratio (TWR) were obtained through measuring the dimensions of the workpiece and the tool stick before and after machining with a dial indicator (803-01, Harbin Measuring and Cutting Tool Group Incorporation, China) and a vernier caliper (202-01, Harbin Measuring and Cutting Tool Group Incorporation, China). The surface roughness (SR Ra) was measured with a surface roughness tester (TR220, Time Group Incorporation, China). The microstructure of the workpiece surface was examined with a scanning electron microscope (SEM, JSM-6380 JEOL, Japan), an X-ray diffraction (XRD, X'Pert PRO MPD, Holland), and an energy dispersive spectrometer (EDS, JED-2300 JEOL, Japan). All the observed specimens had been cleaned ultrasonically and dried with a hot-air blower before the examination.

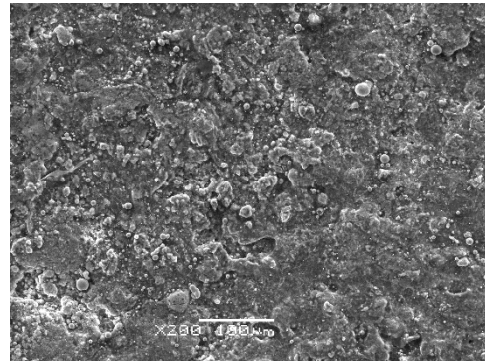
## 4. Results and discussion

### 4.1 Surface morphology of the machined surface

Surface morphology plays an important role in understanding the characteristics of the machined surface. The scanning



(a)



(b)

Fig. 3. SEM micrographs of SiC ceramic surfaces machined by the hybrid process at rough machining mode with different tool polarities under the machining conditions: pulse on-time of 400 μs, pulse off-time of 300 μs, peak voltage of 150V, and peak current of 75 A: (a) Tool (-); (b) Tool (+).

electron microscope (SEM) micrographs of the machined surface at rough machining mode with different tool polarities are illustrated in Fig. 3. The micrographs reveal the appearance of many craters, droplets and cavities on the machined surface when rough machining mode is used. These phenomena point out that the SiC ceramic is molten and/or evaporated by the sparking thermal energy. During machining, sparks are formed at the electrical conductive phase on the SiC ceramic. The discharged energy produces very high temperatures at the point of the spark, causing a minute part of the workpiece to melt and vaporize. When the current flow ceases, a violent collapse of the plasma channel and vapor bubble causes superheated, molten liquids to explode into the gap and the dielectric liquid solidifies the molten material immediately. However, not all of the molten material can be removed because of the surface tension, tensile strength and bonding force between liquid and solid. The molten material remaining on the workpiece surface is rapidly quenched by the emulsion and re-solidifies on the workpiece surface to form droplets. This re-solidifying material simultaneously shrinks after sparking due to the emulsion cooling. Regions where the molten material is re-solidified later on do not have enough molten material to fill in, leading to cavities.

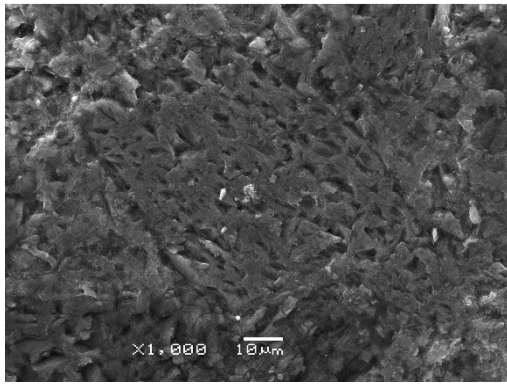


Fig. 4. SEM micrograph of SiC ceramic surface machined by the hybrid process at finish machining mode under the conditions: pulse on-time of 40  $\mu$ s, pulse off-time of 2500  $\mu$ s, peak voltage of 90 V, peak current of 15 A, and positive tool polarity.

It is obvious that the craters and cavities are bigger and deeper in negative tool polarity, whereas the droplets are more in positive tool polarity under the same conditions. During the hybrid process, the tool rotates at a high speed, the discharge point transfer velocity between the electrode and workpiece is very high, and the continuance time of the discharge point between the certain point of the electrode and the certain point of the workpiece is very short. Because the mass of the electrons is much smaller than that of positive ions, and they can be accelerated quickly during a short time, the bombardment effect by electrons is stronger than that by positive ions; therefore, the craters and cavities on the workpiece surface produced by electrons are bigger and deeper. The bombardment effect by positive ions is weaker, so less molten material can be expelled during machining, and more droplets form on the workpiece surface.

The SEM micrograph of the machined surface at finish machining mode is illustrated in Fig. 4. Compared with Fig. 3(b), the machined surface is smooth at finish machining mode and covered by fewer little craters and pockmarks. Moreover, there are some grinding traces on the machined surface, which means that the material is mainly removed by mechanical grinding at finish machining mode.

#### 4.2 Surface roughness

Surface roughness is a critical parameter for evaluating the machined quality. To determine the effect of machining parameters on surface roughness of the SiC ceramic, the arithmetical mean deviation of the profile (Ra) is selected as the surface roughness parameter and is measured by a surface roughness tester through averaging five measurements made stochastically at different positions on the machined surface.

Table 3 shows the experimental results of the surface roughness with different machining conditions. From these results it is obvious that the negative tool polarity causes a poorer surface finish. As mentioned above, the bombardment effect by the electrons is stronger than that by positive ions

Table 3. Process performance and surface composition with different machining conditions.

Pulse on-time ( $\mu$ s)	Pulse off-time ( $\mu$ s)	Peak voltage (V)	Peak current (A)	Tool polarity	MRR ( $\text{mm}^3/\text{min}$ )	SR Ra ( $\mu\text{m}$ )	Fe Mass %	Cu Mass %
400	300	150	75	Negative	130.72	7.62	4.20	4.45
400	300	150	75	Positive	75.75	4.98	12.28	12.50
90	1200	110	45	Negative	33.21	4.28	1.46	1.03
90	1200	110	45	Positive	18.42	2.62	4.58	4.49
120	300	150	75	Negative	110.68	6.69	1.67	1.63
40	300	150	75	Negative	60.84	4.91	1.33	0.94
50	300	150	15	Negative	32.53	4.28	0.21	0.34
50	300	150	45	Negative	62.64	5.56	1.61	1.11

during the hybrid machining of SiC ceramic. Stronger electron bombardment results in bigger and deeper craters, leading to a rougher surface; therefore, the surface roughness is higher in negative tool polarity than that in positive tool polarity.

Table 3 also shows that the SR increases with the increase of pulse on-time and peak current, respectively. This phenomenon can be explained by the correlation between the surface roughness and the machining parameters as follows [19]:

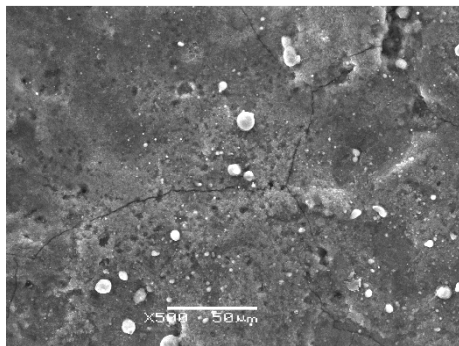
$$R_{\max} = K_R T_{on}^a I_p^b, \quad (1)$$

where  $R_{\max}$  is the surface roughness ( $\mu\text{m}$ ),  $T_{on}$  is the pulse on-time ( $\mu\text{s}$ ),  $I_p$  is the peak current (A),  $K_R$  is the constant, and  $a$ ,  $b$  are the proportional constants. It can be seen from Eq. (1) that under a certain machining condition, the  $R_{\max}$  increases with the increase of pulse on-time and peak current, respectively; therefore, the SR increases.

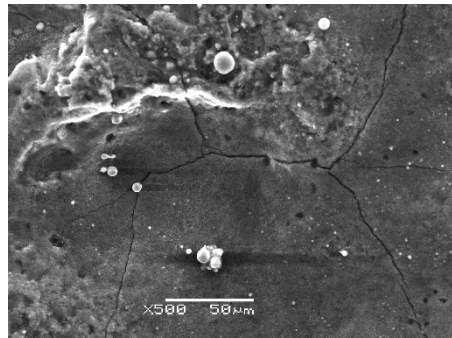
Based on the surface roughness values in Table 3, an excellent machined surface finish can be obtained by setting the machine parameters at a short pulse on-time, a low peak current, and positive tool polarity.

#### 4.3 Micro-cracks on the machined surface

Figs. 5 and 6 show the micro-cracks on the SiC ceramic surfaces machined by the hybrid process under different pulse on-time and peak current settings, respectively. During machining, the thermal impacts of the sparks are accompanied by a very rapid quench rate of the heated material in the plasma contact zone. These thermal waves cause expansion and contraction of re-solidified and heat affected material, which is the main reason for the appearance of the micro-cracks. The SiC ceramic has extreme hardness and brittleness-the gradient of thermal stress is very large during machining, so surface micro-cracks are easily generated on the machined surface. The micro-cracks on the machined surface lead to thermal spalling of the SiC ceramic, so the removal mechanism in the hybrid machining of SiC ceramic consists of not just the melt-



(a)



(b)

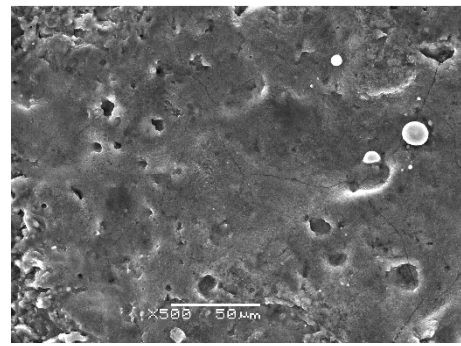
Fig. 5. SEM micrographs showing micro-cracks on the machined surfaces with different pulse on-times under the machining conditions: pulse off-time of 300  $\mu$ s, peak voltage of 150 V, peak current of 75 A, and negative tool polarity: (a) Pulse on-time of 120  $\mu$ s; (b) Pulse on-time of 400  $\mu$ s.

ing and evaporation but also thermal spalling.

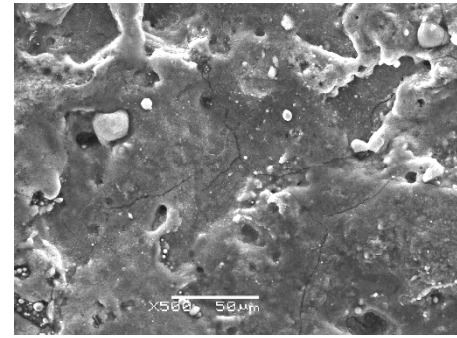
From Figs. 5 and 6 the number and size of the micro-cracks on the machined surface increase with the increase of pulse on-time and peak current, respectively. The phenomenon can be explained as follows. The amount of electrical discharge energy conducted into the machining gap increases with the increase of pulse on-time and peak current, respectively. The energy density of the electrical discharge in the discharge spot on the machined surface increases, and the thermal impact and thermal stress increase, so the number and size of the micro-cracks on the machined surface increase with the increase of pulse on-time and peak current, respectively.

#### 4.4 Compositions of the machined surface

Energy dispersive spectrometer (EDS) spectrum analysis is used to identify the elemental composition on the workpiece surface generated in different machining conditions. Figs. 7 and 8 show the EDS spectrum analysis of the machined surface and the unprocessed surface, respectively. It can be seen from Figs. 7 and 8 that the prominent elements on the machined surface are carbon (C), oxygen (O), silicon (Si), iron (Fe) and copper (Cu), whereas the prominent elements on the unprocessed surface are carbon (C), oxygen (O) and silicon (Si). This means that the migration of material from tool to



(a)



(b)

Fig. 6. SEM micrographs showing micro-cracks on the machined surfaces with different peak currents under the machining conditions: pulse on-time of 50  $\mu$ s, pulse off-time of 300  $\mu$ s, peak voltage of 150 V, and negative tool polarity: (a) Peak current of 15 A; (b) Peak current of 45 A.

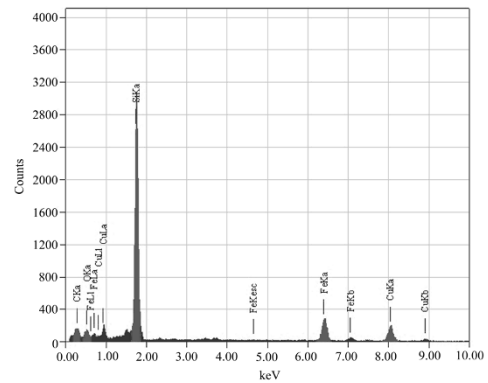


Fig. 7. EDS spectrum analysis of the machined SiC ceramic surface under the machining conditions: pulse on-time of 400  $\mu$ s, pulse off-time of 300  $\mu$ s, peak voltage of 150 V, peak current of 75 A, and positive tool polarity.

workpiece occurs during the hybrid process.

The iron (Fe) percentage and copper (Cu) percentage on the machined SiC ceramic surface with different machining conditions are presented in Table 3. Under the same conditions the metal (Fe and Cu) percentage on the machined surface in positive tool polarity is higher than that in negative tool polarity. This phenomenon can be explained as follows. The electrodes and abrasive sticks contain copper and iron; the elec-

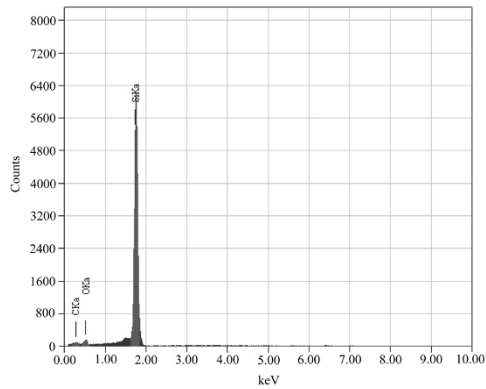


Fig. 8. EDS spectrum analysis of the unprocessed SiC ceramic surface.

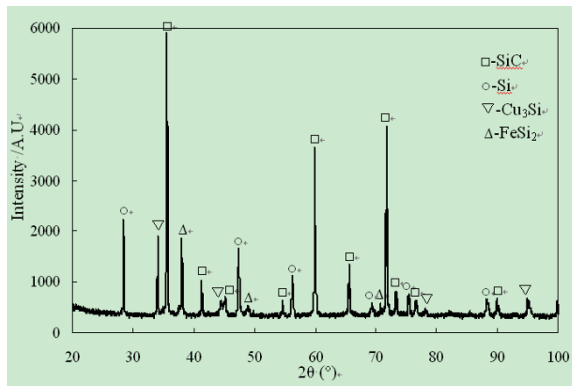


Fig. 9. XRD patterns of SiC ceramic surface machined under the machining conditions: pulse on-time of 400  $\mu$ s, pulse off-time of 300  $\mu$ s, peak voltage of 150 V, peak current of 75 A, and positive tool polarity.

trollysis reaction occurs easily in positive tool polarity under the application of the water-based emulsion, and the removed tool material is mostly ionized into metallic ion, which can attach to the workpiece surface easily. However, the electrolysis reaction occurs difficultly in negative tool polarity because the SiC is a nonmetal. Therefore, the metal percentage on the machined surface is high in positive tool polarity.

Also from Table 3 the metal percentage on the machined surface increases with the increase of pulse on-time and peak current, respectively. This is because the single pulse energy, thermal energy density and discharge explosive force increase with the increase of pulse on-time and peak current, respectively. Tool material removal is enhanced, and more tool material can transfer to the workpiece surface; therefore, the metal percentage on the machined surface increases.

To study the phase change that has occurred during the hybrid process, the X-ray diffraction (XRD) patterns of the machined surface and the unprocessed surface are presented in Figs. 9 and 10, respectively. The prominent substances on the machined surface are copper silicide ( $\text{Cu}_3\text{Si}$ ), iron silicide ( $\text{FeSi}_2$ ), silicon (Si), and silicon carbide (SiC), whereas the prominent substances on the unprocessed surface are silicon (Si), and silicon carbide (SiC). This indicates that copper silicide ( $\text{Cu}_3\text{Si}$ ) and iron silicide ( $\text{FeSi}_2$ ) are generated during the

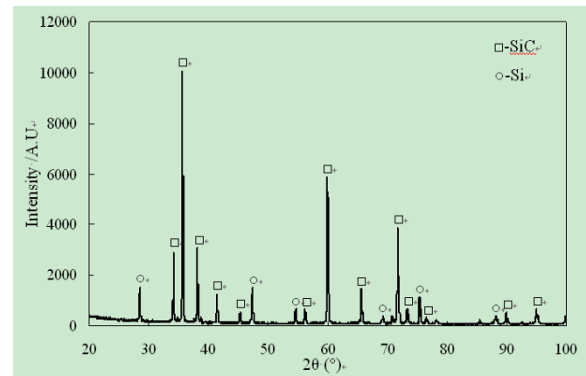


Fig. 10. XRD patterns of unprocessed SiC ceramic surface.

hybrid machining of SiC ceramic. It can be concluded that a modified layer forms on the machined surface, and a combination reaction takes place during the hybrid machining of SiC ceramic, which can be described as follows:



## 5. Conclusions

(1) A novel high speed hybrid machining process that integrates end electric discharge (ED) milling and mechanical grinding to machine SiC ceramic is proposed. The process employs a water-based emulsion as the machining fluid, and it shows high machining efficiency, good surface quality and fine working environmental practice.

(2) When rough machining mode is used, the machined surface is rough, and the craters and cavities are bigger and deeper in negative tool polarity, whereas the droplets are more in positive tool polarity under the same conditions on the machined surface. When finish machining mode is used, the machined surface is smooth and covered by fewer little craters and pockmarks. Moreover, SiC ceramic is mainly removed by end ED milling such as melting, evaporation and thermal spalling at rough machining mode, whereas it is mainly removed by mechanical grinding at finish machining mode.

(3) As the pulse on-time and peak current increase, respectively, the surface roughness and the number and size of the micro-cracks on the machined surface increase. Furthermore, the surface roughness is higher in negative tool polarity than that in positive tool polarity. Therefore, the positive tool polarity, the short pulse on-time, and the low peak current cause a fine surface finish.

(4) The chemical compositions of the machined surface differ from the unprocessed surface due to the diffusion of the tool material, and a combination reaction takes place during machining. Furthermore, the tool material that is transferred to the workpiece surface increases with the increase of pulse on-time and peak current, respectively, and more tool material can transfer to the workpiece surface in case of positive tool polarity, when compared to negative tool polarity under the same conditions.



## Acknowledgments

The work is partially supported by a grant from the National Natural Science Foundation of China (Grant No. 51205411), a grant from Shandong Provincial Natural Science Foundation of China (Grant No. ZR2012EEL15), and a grant from the Fundamental Research Funds for the Central Universities (Grant No. 11CX04031A).

## References

- [1] A. Okada, Automotive and industrial applications of structural ceramics in Japan, *Journal of the European Ceramic Society*, 28 (5) (2008) 1097-1104.
- [2] Y. Kato, S. Kondo and L. L. Snead, DC electrical conductivity of silicon carbide ceramics and composites for flow channel insert applications, *Journal of Nuclear Materials*, 386-388 (C) (2009) 639-642.
- [3] H. T. Bae, H. J. Choi, J. H. Jeong and D. S. Lim, The effect of reaction temperature on the tribological behavior of the surface modified silicon carbide by the carbide derived carbon process, *Materials and Manufacturing Processes*, 25 (5) (2010) 345-349.
- [4] X. Guo, H. Yang, L. Zhang and X. Zhu, Sintering behavior, microstructure and mechanical properties of silicon carbide ceramics containing different nano-TiN additive, *Ceramics International*, 36 (1) (2010) 161-165.
- [5] A. V. Gopal and P. V. Rao, A new chip-thickness model for performance assessment of silicon carbide grinding, *International Journal of Advanced Manufacturing Technology*, 24 (11-12) (2004) 816-820.
- [6] S. Agarwal and P. V. Rao, Grinding characteristics, material removal and damage formation mechanisms in high removal rate grinding of silicon carbide, *International Journal of Machine Tools and Manufacture*, 50 (12) (2010) 1077-1087.
- [7] F. L. Zhang, Machining mechanism of abrasive water jet on ceramics, *Key Engineering Materials*, 426-427 (2010) 212-215.
- [8] A. N. Samant and N. B. Dahotre, Laser machining of structural ceramics-A review, *Journal of the European Ceramic Society*, 29 (6) (2009) 969-993.
- [9] N. J. Churi, Z. J. Pei, D. C. Shorter and C. Treadwell, Rotary ultrasonic machining of silicon carbide: Designed experiments, *International Journal of Manufacturing Technology and Management*, 12 (1-3) (2007) 284-298.
- [10] M. Gostimirovic, P. Kovac, M. Sekulic and B. Skoric, Influence of discharge energy on machining characteristics in EDM, *Journal of Mechanical Science and Technology*, 26 (1) (2012) 173-179.
- [11] M. Shabgard, S. N. B. Oliaei, M. Seyedzavvar and A. Najadebrahimi, Experimental investigation and 3D finite element prediction of the white layer thickness, heat affected zone, and surface roughness in EDM process, *Journal of Mechanical Science and Technology*, 25 (12) (2011) 3173-3183.
- [12] G. S. Prihandana, M. Mahardika, M. Hamdi and K. Mitsui, Effect of low-frequency vibration on workpiece in EDM processes, *Journal of Mechanical Science and Technology*, 25 (5) (2011) 1231-1234.
- [13] R. Ji, Y. Liu, Y. Zhang and F. Wang, Machining performance of silicon carbide ceramic in end electric discharge milling, *International Journal of Refractory Metals and Hard Materials*, 29 (1) (2011) 117-122.
- [14] F. Z. Han, Y. X. Wang and M. Zhou, High-speed EDM milling with moving electric arcs, *International Journal of Machine Tools and Manufacture*, 49 (1) (2009) 20-24.
- [15] Y. H. Liu, R. J. Ji, Q. Y. Li, L. L. Yu and X. P. Li, An experimental investigation for electric discharge milling of SiC ceramics with high electrical resistivity, *Journal of Alloys and Compounds*, 472 (1-2) (2009) 406-410.
- [16] R. Ji, Y. Liu, Y. Zhang, B. Cai, H. Li and J. Ma, Optimizing machining parameters of silicon carbide ceramics with ED milling and mechanical grinding combined process, *International Journal of Advanced Manufacturing Technology*, 51 (1-4) (2010) 195-204.
- [17] R. J. Ji, Y. H. Liu, Y. Z. Zhang, H. Li and X. D. Cheng, Machining performance and surface integrity of SiC ceramic machined using electrical discharge milling and the mechanical grinding compound process, *Proceedings of the Institution of Mechanical Engineers, Part B: Journal of Engineering Manufacture*, 224 (10) (2010) 1511-1518.
- [18] N. F. Petrofes and A. M. Gadalla, Electrical discharge machining of advanced ceramics, *American Ceramic Society Bulletin*, 67 (6) (1988) 1048-1052.
- [19] J. C. Liu, J. C. Bai and Y. F. Guo, *Non-Traditional Machining*, Fifth Ed. China Machine Press, Beijing, People's Republic of China (2009).



His recent research interest is electrical discharge machining of engineering ceramics.



His research fields include electrical discharge machining of engineering ceramics, expansion sand screen for sand control and control system of subsea drilling equipment.

**Renjie Ji** received his Ph.D in Electromechanics Engineering from China University of Petroleum in 2011. Currently, he is a lecturer in the College of Electromechanical Engineering, China University of Petroleum, China. He has published over 40 papers in international or national journals and conferences.

**Yonghong Liu** received his Ph.D in Mechanical Manufacture from Harbin Institute of Technology, Harbin, China, in 1996. Currently, he is a professor and doctoral supervisor in the College of Electromechanical Engineering, China University of Petroleum, China. He has published over 120 papers in international or national journals and conferences.